Symmetric splitting of very light systems

K. Grotowski, Z. Majka, R. Płaneta, and M. Szczodrak
Institute of Physics, Jagellonian University, Reymonta 4, Cracow, Poland

Y. Chan, G. Guarino,* L. G. Moretto, D. J. Morrissey,† L. G. Sobotka,‡ R. G. Stokstad, I. Tserruya,§ S. Wald, and G. J. Wozniak
Nuclear Science Division, Lawrence Berkeley Laboratory, University of California, Berkeley, California 94720
(Received 11 June 1984)

Inclusive and coincidence measurements have been performed to study symmetric products from the reactions 74–186 MeV $^{12}C+^{40}Ca$, 141 MeV $^{9}Be+^{40}Ca$, and 153 MeV $^{6}Li+^{40}Ca$. The binary decay of the composite system has been verified. Energy spectra, angular distributions, and fragment correlations are presented. The total kinetic energies for the symmetric products from these very light composite systems are compared to liquid drop model calculations and fission systematics.

I. INTRODUCTION

Fission reactions that produce fragments close to one-half the mass of the composite system are traditionally observed in heavy nuclei. In light systems, symmetric splitting is rarely observed and poorly understood.

The distribution of products from the decay of a compound system is expected to depend significantly on the mass A, atomic number Z, and angular momentum l of the system. The potential energy varies dramatically with the exit channel mass asymmetry as the fissility parameter x crosses a critical value at $x=0.396$ (the Businaro-Gallone limit[1]). For $A \gtrsim 100$ and $l=0$, x is larger than the Businaro-Gallone limit. A minimum in the potential energy is present at symmetry and as a consequence such reactions should exhibit a maximum yield at symmetry.[2–4] For $A \lesssim 100$ and $l=0$, x becomes equal to or smaller than the Businaro-Gallone limit. A maximum in the potential energy is present at symmetry and consequently such reactions should exhibit a minimum at symmetry. A peak in the yield at symmetry for such light systems would imply some amount of angular momentum,[2] which moves the Businaro-Gallone point toward smaller values of x.

In view of the above considerations, it would be interesting to verify the existence of the symmetric splitting of compound nuclei with fissility parameters less than the Businaro-Gallone limit. For systems with $A<80$, evidence for possible symmetric splitting has been observed in only a few inclusive measurements.[5–8] In the reaction 150 MeV $^{4}He+^{45}Sc$, David *et al.*[6] observed a significant yield of ^{24}Na activity and suggested that this may represent a fission product. More recently,[8] products with about half the mass of the compound system were observed in the reaction 156 MeV $^{6}Li+^{40}Ca$. Because the above studies were inclusive measurements, the presence of products with about one-half the mass of the compound nucleus does not prove the existence of a fission process. In particular, these light compound nuclei were typically formed with sufficient excitation energy to undergo large mass loss due to successive α-particle evaporation. Furthermore, reactions on light target contaminants can produce products with masses near $A=20$.

To demonstrate symmetric splitting for these highly excited light systems ($A\sim 50$), it is essential to show in a coincidence experiment that there are two fragments, each having approximately one-half the mass of the compound nucleus. It is also important to minimize the production of symmetric fragments via a deep inelastic mechanism by choosing reactions with a large entrance channel mass asymmetry. To this end, the kinetic energy spectra and the in-plane angular correlation of symmetric products were measured for the following reactions: 121 and 186 MeV $^{12}C+^{40}Ca$, 141 MeV $^{9}Be+^{40}Ca$, and 153 MeV $^{6}Li+^{40}Ca$. The out-of-plane correlation of symmetric products was also measured for the reaction 186 MeV $^{12}C+^{40}Ca$. Table I presents some characteristic parameters of these systems. The coincidence measurements of the $^{12}C+^{40}Ca$ system demonstrated that essentially all of the inclusive yield of symmetric products around 40° results from a binary decay. To characterize the dependence of the symmetric splitting process on the excitation energy of the $^{12}C+^{40}Ca$ system, inclusive measurements were made at bombarding energies of 74, 132, 162, and 185 MeV.

Unfortunately, for such light systems, the primary fragments are highly excited and lose a significant fraction of their mass, charge, energy, and momentum by sequential particle emission. This makes the transformation of the laboratory data to the primary, preevaporative system difficult if not impossible. For this reason, comparisons

TABLE I. Some parameters which characterize the reaction systems investigated in this work.

Reaction	E_{lab} (MeV)	$E_{c.m.}$ (MeV)	$\frac{A_T-A_p}{A_T+A_p}$	Fissility
$^{12}C+^{40}Ca\rightarrow^{52}Fe^*$	186	143	0.54	0.25
$^{9}Be+^{40}Ca\rightarrow^{49}Cr^*$	141	115	0.63	0.23
$^{6}Li+^{40}Ca\rightarrow^{46}V^*$	153	133	0.74	0.23

with reaction models were made in the laboratory system after applying a Monte Carlo simulation of the effects of particle evaporation.

II. EXPERIMENTAL METHOD AND DATA

Beams of ^{6}Li, ^{9}Be, and ^{12}C ions from the Lawrence Berkeley Laboratory 88-inch Cyclotron were used to bombard a 0.40 mg/cm^2 self-supporting target of natural calcium. The reaction products were detected in ΔE-E (gas-silicon) telescopes placed on movable arms. The circular entrance windows of the telescopes subtended solid angles of $\sim$7 msr, determined for each telescope by an ^{241}Am source of known activity placed in the target position. Small permanent magnets were mounted in front of the telescopes to suppress secondary electrons.

The energy scale (E) was calibrated at low energies with a ^{212}Pb source and at high energies by ^{12}C, ^{16}O, and ^{20}Ne ions (75, 100, and 125 MeV, respectively) elastically scattered from a thin gold target. The linearity of the scale was checked with a precision pulser. The ΔE energy scale was calibrated by measuring the shift of the energy peaks in the E detector and the corresponding amplitude in the ΔE detector for runs with and without gas in the telescope. Energy losses by the reaction products in the target and in the telescope windows were taken into account.

Time correlations between the telescopes were measured with a time-to-amplitude converter (TAC). The random coincidences were a small fraction of the real coincidences. In measurements where singles and coincidence data were recorded simultaneously, the singles data were scaled down by a factor of 32 or 64. The E, ΔE, and TAC signals were digitized by a 4096-channel analog-to-digital converter and were written event by event on magnetic tape.

A. Singles data

A typical E vs ΔE map for products from the reaction 186 MeV ^{12}C+^{40}Ca is shown in Fig. 1. Ridges are seen corresponding to elements with atomic numbers up to Z=20. The absolute Z calibration was provided by the intense projectile ridge and the ^{7}Be,^{9}Be doublet. For Z values larger than 14, there is a loss of elemental resolution in the energy region below the Bragg peak. Different regions of the E-ΔE map are populated with different intensities (see Fig. 1). In the present work we shall concentrate on studying the weakly populated, nearly-symmetric region ($Z \approx 9$–11).

Representative laboratory energy spectra for nearly-symmetric products are presented in Fig. 2. To improve statistics, products with Z=9–11 and 8–10 were summed together for the ^{12}C+^{40}Ca and ^{6}Li,^{9}Be+^{40}Ca systems, respectively. These spectra were generated by setting two-dimensional free form gates around the corresponding element ridges shown in Fig. 1. Because individual elements are not resolved at low energies, an energy cutoff was set at about 15 MeV. Most of the energy spectrum is above this cutoff for the ^{12}C+^{40}Ca reaction [Fig. 2(a)]; however, the peak region is not as well characterized for the ^{6}Li,^{9}Be+^{40}Ca reactions. The effect of the energy cutoff increases with the increasing laboratory angle. The error bars shown in Fig. 2 and in the following figures reflect only the statistical uncertainties.

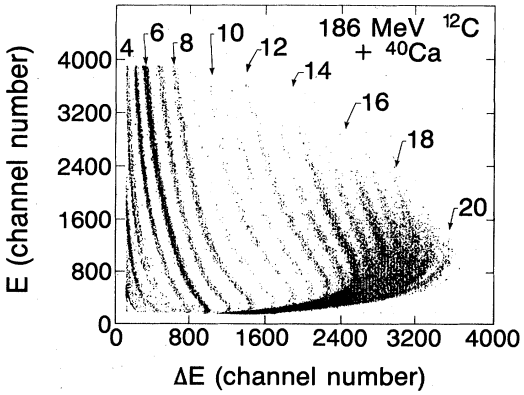

FIG. 1. An E vs ΔE map for angle-integrated (θ_{lab}=20°–70°) reaction products from the 186 MeV ^{12}C+^{40}Ca reaction illustrating the elemental resolution of the ΔE-E telescopes.

Representative energy-integrated Z distributions are

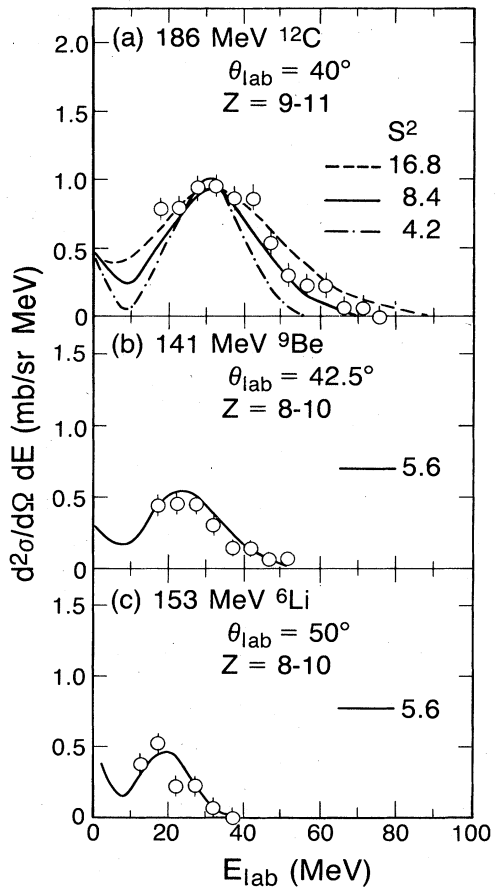

FIG. 2. Representative laboratory energy spectra (symbols) for symmetric products from the (a) 186 MeV ^{12}C, (b) 141 MeV ^{9}Be, and (c) 153 MeV ^{6}Li+^{40}Ca reactions. The curves are Monte Carlo calculations for different values of S^2 (in units of 10^{-5} c^2), the variance of the c.m. velocity distribution (see the text).

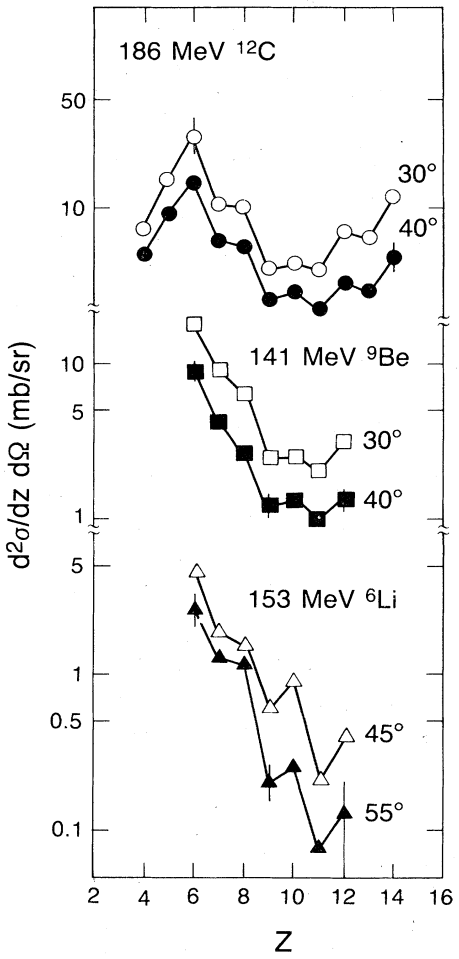

FIG. 3. Representative energy-integrated charge distributions of products from three reactions on a ^{40}Ca target: 186 MeV ^{12}C, 141 MeV ^{9}Be, and 153 MeV ^{6}Li. The data have not been corrected for the experimental low energy cutoff.

displayed in Fig. 3. For all three reactions there is about an order of magnitude decrease in yield between $Z=6$ and 9. All systems exhibit a weak odd-even effect[9] that is strongest for the $^{12}C+^{40}Ca$ system. In this latter case there is a minimum in yield, slightly below the Z value corresponding to a symmetric disintegration. For the $^{9}Be+^{40}Ca$ system, the yields fluctuate around a more or less constant average value for $Z \geq 9$ whereas for the $^{6}Li+^{40}Ca$ system the yield decreases with increasing Z value.

Inclusive laboratory angular distributions for $Z=10$ and 11 from the $^{12}C+^{40}Ca$ system are shown in Fig. 4 for several bombarding energies between 74 and 185 MeV. At all bombarding energies, the angular distributions are forward peaked and the degree of forward peaking increases with decreasing bombarding energy. At all angles the yield decreases with decreasing bombarding energy. However, at larger angles (40°–60°) the decrease in yield is much more rapid and falls by more than an order of magnitude over the measured range of bombarding energies.

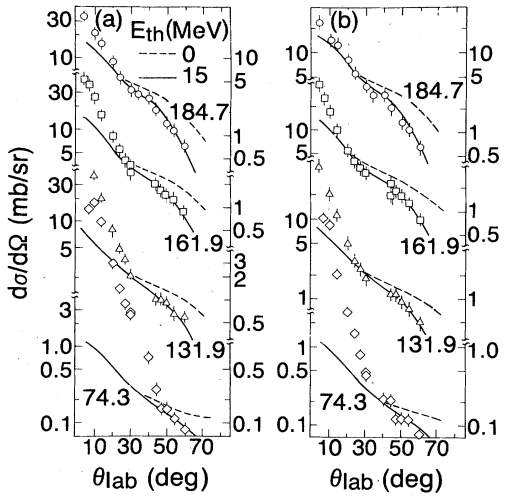

FIG. 4. Inclusive laboratory angular distributions for typical symmetric products (a) $Z=10$ and (b) $Z=11$ from the $^{12}C+^{40}Ca$ reaction at several bombarding energies. The curves are Monte Carlo angular distributions calculated with (solid) and without (dashed) the experimental energy cutoff (see discussion in the text). Experimental cross sections corrected for the low energy cutoff can be obtained by multiplying each data point by the ratio of the dashed to solid curves.

B. Coincidence data

Energy- and angle-integrated charge distributions for Z_1-Z_2 coincidences are presented in Fig. 5 for the 186 MeV $^{12}C+^{40}Ca$ reaction. For this system the bulk of the events are spread along a diagonal line with $Z_1+Z_2 \sim 20$. The diagonal line given by $Z_1+Z_2=Z_p+Z_T=26$ corresponds to binary reactions with no subsequent charged-particle evaporation. Here Z_p, Z_T, Z_1, and Z_2 denote, respectively, the atomic numbers of the projectile, target, and of the fragments detected in the two telescopes. Thus, the line defined by $Z_1+Z_2=20$ represents an average missing charge ΔZ of 6, which is most likely lost

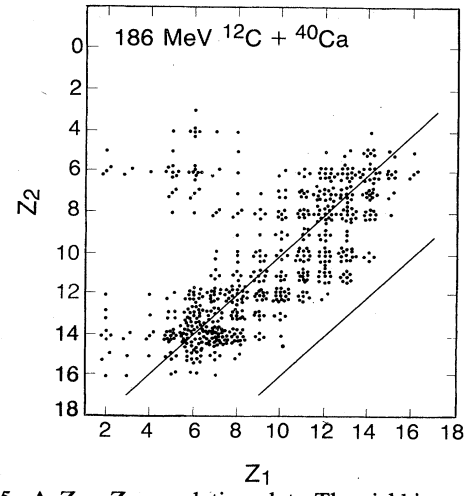

FIG. 5. A Z_1-Z_2 correlation plot. The yield is proportional to the density of dots (see the text). The upper and lower lines correspond to $Z_1+Z_2=20$ and $Z_1+Z_2=26$, respectively.

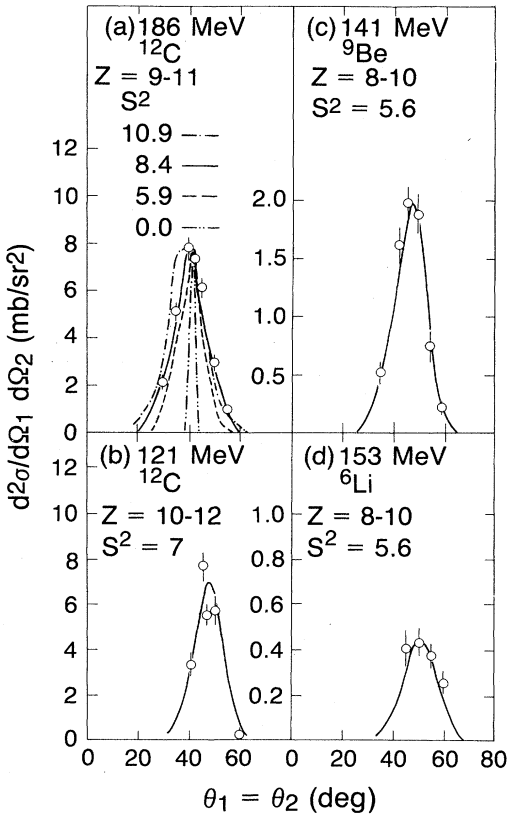

FIG. 6. In-plane angular correlation ($\theta_1=\theta_2$) of symmetric products ($Z_1=Z_2$) for four systems: (a) 186 MeV ^{12}C, (b) 121 MeV ^{12}C, (c) 141 MeV ^{9}Be, and (d) 153 MeV ^{6}Li+^{40}Ca. The values of Z_1 summed together are the following: 9—11, 10—12, 8—10, and 8—10, respectively. The data have not been corrected for the low energy cutoff. The curves are Monte Carlo calculations for different values of S^2 (in units of 10^{-5} c^2, see the text) and primary c.m. kinetic energies of the symmetric fragments of (a) 16.7 MeV, (b) 17.3 MeV, (c) 15.0 MeV, and (d) 14.3 MeV. The shape of the calculated curves is unaffected by the low energy cutoff.

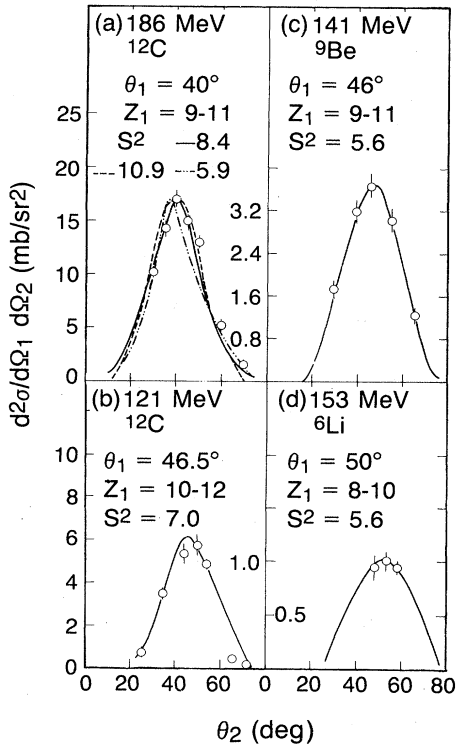

FIG. 7. In-plane angular correlation of symmetric products from a ^{40}Ca target for fixed θ_1 and the Z_2 gate wide enough to accept all residues of the complimentary fragments: (a) 186 MeV ^{12}C, $\theta_1=40°$; (b) 121.2 MeV ^{12}C, $\theta_1=46.5°$; (c) 141 MeV ^{9}Be, $\theta_1=46°$; and (d) 153 MeV ^{6}Li, $\theta_1=50°$. The curves are Monte Carlo calculations for the same parameters used in Fig. 6.

through particle evaporation from the excited primary fragments.

The yield for equal values of Z_1 and Z_2 clearly demonstrates the existence of symmetric and nearly symmetric splitting of these light systems with $A\sim50$. It appears that the symmetric products have a somewhat smaller total charge loss than the asymmetric splits (see Fig. 5). For the ^{12}C+^{40}Ca system, the average charge loss decreases from six to four charge units when the bombarding energy is lowered from 186 to 121 MeV. The average missing charges for the 153 MeV ^{6}Li+^{40}Ca and the 141 MeV ^{9}Be+^{40}Ca systems are 5 and 4, respectively.

In Fig. 6 are shown the in-plane angular correlations of symmetric products for four systems measured with two telescopes at equal angles on opposite sides of the beam. The angular correlations are peaked at angles between 40°—50° and have a significant width. As is expected for a binary process, the mean angle of the correlation increases as the bombarding energy and projectile mass decrease. In Sec. III it is shown that the mean angle for symmetric splitting is also simply related to the total kinetic energy in the c.m. system. For the ^{12}C+^{40}Ca system the yield of symmetric products decreases slightly as the bombarding energy decreases from 186 to 121 MeV. However, the yield of symmetric products decreases by more than an order of magnitude as the entrance channel asymmetry increases from ^{12}C+^{40}Ca to ^{6}Li+^{40}Ca. This strong decrease is somewhat moderated (see Sec. III) after applying the larger energy cutoff corrections for the ^{6}Li+^{40}Ca data.

The in-plane angular correlation data in Fig. 7 were measured by placing one of the telescopes at the angle (θ_{ss}) of the maximum coincidence yield and varying the angle of the second telescope. To facilitate comparison of the inclusive and coincidence data, the data in Fig. 7 include coincidences between symmetric products ($Z=9$—11) and all residues ($Z=8$—14) of the complementary fragments (see Fig. 5). These in-plane correlation functions are quite broad, and may result from both Q-value fluctuations at the saddle point and evaporation of particles from the excited primary reaction products.

A coarse out-of-plane correlation function was measured with one telescope fixed in the reaction plane, at $\theta_1=\theta_{ss}$ (at the azimuthal angle $\phi=0°$) and three others placed in the plane perpendicular to the reaction plane and located on the opposite side of the beam, also at $\theta_2=\theta_{ss}$. Coincidence data were taken between the in-

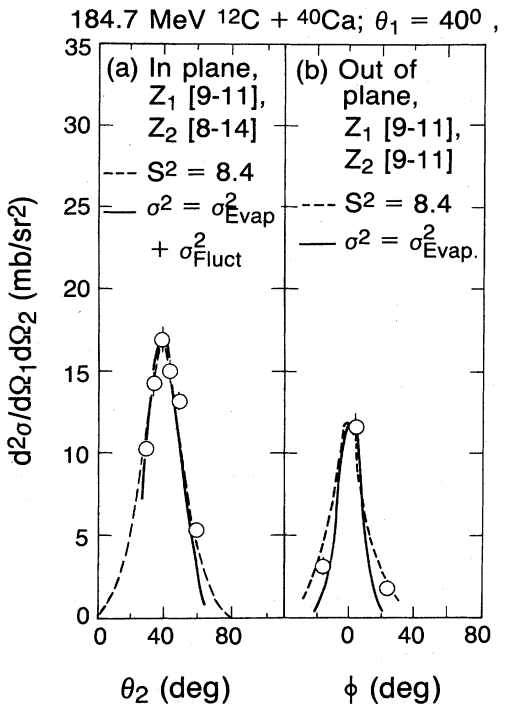

FIG. 8. Measured (a) in-plane correlation and (b) out-of-plane correlation for the $^{12}C+^{40}Ca$ system. The solid curve is a Gaussian which includes contributions to its width from σ_{evap} and σ_{fluct} (see discussion in the text). The dashed curve is a Monte Carlo calculation with $S^2=8.4\times10^{-5}$ c^2 and $E'^{c.m.}_{kin}=16.7$ MeV.

plane telescope and each out-of-plane telescope. Due to the low coincidence counting rates and the limited amount of beam time available, the out-of-plane correlation curve contains only three experimental points (Fig. 8). The above angular correlation measurements clearly demonstrate the existence of symmetric and nearly symmetric splitting in systems with $A\sim50$.

III. MONTE CARLO CALCULATION AND RESULTS

It is an open question whether evaporation occurs before as well as after the splitting of the compound nucleus. We assume in this work the formation of a compound system followed by a first chance binary splitting and, afterwards, evaporation of light particles from the excited fragments. This is based on the assumption that first chance evaporation and the corresponding loss of angular momentum should reduce considerably the probability of symmetric splitting. However, one cannot exclude some contribution from prescission evaporation.

The following reaction picture has been adopted. In a collision of a projectile p with a target nucleus T, two highly excited fragments are produced. As a result of evaporation, the secondary fragments have different directions, energies, and atomic and mass numbers than the primary products. All the reaction parameters and cross sections before evaporation are denoted by primed symbols and after evaporation by unprimed ones.

A. Monte Carlo calculation

An event-by-event transformation from the secondary reaction products (observed in the laboratory system) to the primary reaction products is made impossible by the evaporation of particles that are not observed in the experiment. Therefore, the primary symmetric splitting of the composite system and the subsequent velocity change due to secondary evaporation have been simulated using the Monte Carlo method. The calculations were performed in velocity space (see Fig. 9) where $\vec{V}_0$ is the velocity of the composite system and $\vec{V}'_{c.m.}$ denotes the initial center-of-mass (c.m.) velocity of each fragment. A symmetric mass split was assumed. A random number generator gave the initial directions of the fragments according to an assumed c.m. angular distribution ($d\sigma/d\Omega\sim1/\sin\theta_{c.m.}$). To determine the average recoil velocities for both fragments ($\vec{v}^{\,1}_{recoil}$ and $\vec{v}^{\,2}_{recoil}$), a Gaussian probability distribution was assumed for each Cartesian component of $\vec{v}_{recoil}$ with a variance S^2 (see Ref. 10). The final velocity of a fragment is given by

$$\vec{V}_i=\vec{V}_0+(-1)^{i+1}\vec{V}'_{c.m.}+\vec{v}^{\,i}_{recoil}\,, \tag{1}$$

where $i=1$ or 2, respectively.

In order to obtain the final laboratory energy of a fragment one has to know its velocity after evaporation. Two approximations were made: an isotropic distribution of recoil velocities was assumed ($\vec{v}^{\,i}_{recoil}$) and the velocity distribution for the fission fragments in the c.m. was replaced by an average value $V'_{c.m.}$. One can argue that the recoil velocity distribution is not isotropic, as the intrinsic spin of the fragments should give some focusing in the reaction plane, particularly for evaporated α particles. However, the intrinsic spin of the symmetric fragments takes no more than $\frac{1}{7}$ of the entrance channel angular momentum. This gives only about $7\hbar$ units per fragment. Since at the scission point the fragments are probably deformed, the actual fragment spin is probably smaller, and this suggests that the isotropic approximation is reasonable. The mass of the fragment was assumed to be twice its atomic number.

The Q-value fluctuations at the scission point give a distribution of the c.m. kinetic energies around the average value $E'^{c.m.}_{kin}$. This effect contributes to the width of both the energy and the angular distributions (angular

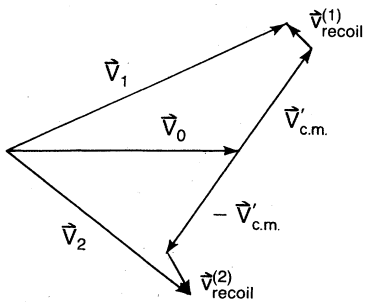

FIG. 9. A velocity vector diagram of the symmetric decay process showing the effect of particle evaporation on the secondary velocities.

correlations) observed in the laboratory system.[2] Let σ_{evap} be the variance of the angular correlation between the fragments caused by evaporation, and let σ_{fluct} denote the corresponding variance due to the Q-value fluctuations. One obtains for the ratio of the out-of-plane to the in-plane widths

$$\sigma_{\text{evap}}/(\sigma_{\text{evap}}^2+\sigma_{\text{fluct}}^2)^{1/2}=0.84$$

for the $^{12}C+^{40}Ca$ system. Here we have made use of the formula given for σ_{evap} by Sikkeland and Viola[11] (after some modification), and for σ_{fluct} by Moretto.[2]

In Fig. 8 the in-plane and out-of-plane correlations are estimated with Gaussian functions (solid curve) having variances

$$\sigma=(\sigma_{\text{evap}}^2+\sigma_{\text{fluct}}^2)^{1/2}$$

and σ_{evap}, respectively. The agreement between the data points and the solid curves is reasonable. A Monte Carlo calculation (dashed curves) which includes the detector acceptance angles gives somewhat better agreement with the experimental data.

This estimated ratio of the in-plane to out-of-plane widths results in a 16% correction in the evaluation of the cross section (Sec. III C) but does not change the corrections for the energy threshold nor the evaluation of $E'^{\text{c.m.}}_{\text{kin}}$ (Sec. III B). The corresponding corrections are comparable (22% and 16%) for the $^{9}Be+^{40}Ca$ and the $^{6}Li+^{40}Ca$ systems, respectively.

Following the Monte Carlo procedure one can generate the energy spectra of particles and simulate event by event the number of singles and coincidences detected above some energy cutoff at different laboratory angles. In this way one can predict the shapes of both singles angular distributions and coincidence correlation functions measured in the laboratory system above the experimental energy cutoff

$$[N_{\text{singles}}(\theta,\phi)]_{\text{MC}}=\frac{N}{\sigma_f}\left[\frac{d\sigma}{d\Omega}(\theta,\phi)\right]_{\text{MC}}\Delta\Omega\,, \tag{2}$$

$$[N_{\text{coinc}}(\theta_1,\theta_2,\phi_1,\phi_2)]_{\text{MC}}=\frac{N}{\sigma_f}\left[\frac{d^2\sigma(\theta_1,\theta_2,\phi_1,\phi_2)}{d\Omega_1 d\Omega_2}\right]_{\text{MC}}\Delta\Omega_1\Delta\Omega_2\,. \tag{3}$$

Here, $[d\sigma/d\Omega]_{\text{MC}}$ is the differential cross section assumed in the Monte Carlo calculation; σ_f is the total cross section for a symmetric mass split having the angular distribution $[d\sigma/d\Omega]_{\text{MC}}$; $\Delta\Omega$, $\Delta\Omega_1$, and $\Delta\Omega_2$ are the solid angles of the detectors; and N is the number of Monte Carlo drawings. If proper values are chosen for $E'^{\text{c.m.}}_{\text{kin}}$, S^2, $d\sigma/d\Omega$, and for the experimental energy cutoffs, then

$$[N_{\text{singles}}(\theta,\phi)]_{\text{exp}}=[N_{\text{singles}}(\theta,\phi)]_{\text{MC}}$$

and (4)

$$[N_{\text{coinc}}(\theta_1,\theta_2,\phi_1,\phi_2)]_{\text{exp}}=[N_{\text{coinc}}(\theta_1,\theta_2,\phi_1,\phi_2)]_{\text{MC}}\,.$$

In this case, the value of σ_f assumed in the Monte Carlo calculation is the best estimate of the true cross section.

The predictions of the Monte Carlo simulation are compared to experimental data in Fig. 2 (energy spectra), and in Figs. 6 and 7 (angular correlations). For reasonable values of S^2 the agreement is good. Calculations were performed for a number of different values of S^2 and showed that the angular correlation data are more sensitive to S^2 than are the energy spectra. The best fit values of S^2 are listed in Table II. The S^2 values are similar for the $^{12}C+^{40}Ca$ system at both bombarding energies. At other bombarding energies, linearly interpolated (or extrapolated) values of S^2 were used.

TABLE II. The values of S^2 and $E'^{\text{c.m.}}_{\text{kin}}$ values obtained from the singles and coincidence measurements.

Reaction	S^2 ($\times10^{-5}$ c^2)	$E'^{\text{c.m.}}_{\text{kin}}$ (MeV) (singles)	$E'^{\text{c.m.}}_{\text{kin}}$ (MeV) (coincidence)
$^{12}C+^{40}Ca$, 186 MeV	8.4	16.7±1	15.1
121.2 MeV	7.0	17.3±1.5	17.0
$^{9}Be+^{40}Ca$, 141 MeV	5.6	15.0±2.5	14.8
$^{6}Li+^{40}Ca$, 153 MeV	5.6	14.3±3.5	14.5

The value of S^2 for the reaction $^{12}C+^{40}Ca$ which gives the best agreement with the data is $\sim8\times10^{-5}$ c^2; the excitation energy of each primary fragment (^{26}Al) is centered at about 50 MeV for the 186 MeV bombarding energy. A comparison of these extracted widths, S^2, can be made with those obtained from the decay of ^{26}Al formed by the fusion of $^{12}C+^{14}N$ (Ref. 10). The corresponding widths for evaporation residues of $Z=10$ in this case are 4×10^{-5} c^2 at $E^*=40$ MeV and 29×10^{-5} c^2 at $E^*=83$ MeV. Thus, these values bracket those obtained in fitting the binary reaction products from the $^{12}C+^{40}Ca$ reaction.

As seen in Figs. 4 and 10(a), the Monte Carlo predictions (solid lines) agree well with the 186 MeV $^{12}C+^{40}Ca$ angular distributions, except at laboratory angles smaller than about 25° where a more forward peaked component is seen. This component becomes stronger when the incident ^{12}C energy decreases. For the 74 MeV $^{12}C+^{40}Ca$ and the $^{6}Li,^{9}Be+^{40}Ca$ systems, it extends out to an angle of about 40°.

It should be pointed out that in the Monte Carlo calculations a $1/\sin\theta_{\text{c.m.}}$ shape of the angular distribution was assumed for the primary fragments, and that this resulted in a good agreement with experimental data over a quite wide range of laboratory angles. For the 185 MeV $^{12}C+^{40}Ca$ system and $Z=11$ this range is from 20° to 60°. After taking into account the evaporation effects this corresponds roughly to a range of c.m. angles of 45°–115°.

B. c.m. kinetic energy of the fragments

For a symmetric mass split, the primary reaction angle θ'_{ss} is simply related to $E'^{\text{c.m.}}_{\text{kin}}$ by

$$E'^{\text{c.m.}}_{\text{kin}}=\frac{1}{2}\frac{A_p}{A_p+A_T}E_p\tan^2\theta'_{ss}\,, \tag{5}$$

here A_p and A_T denote the mass numbers of the projectile

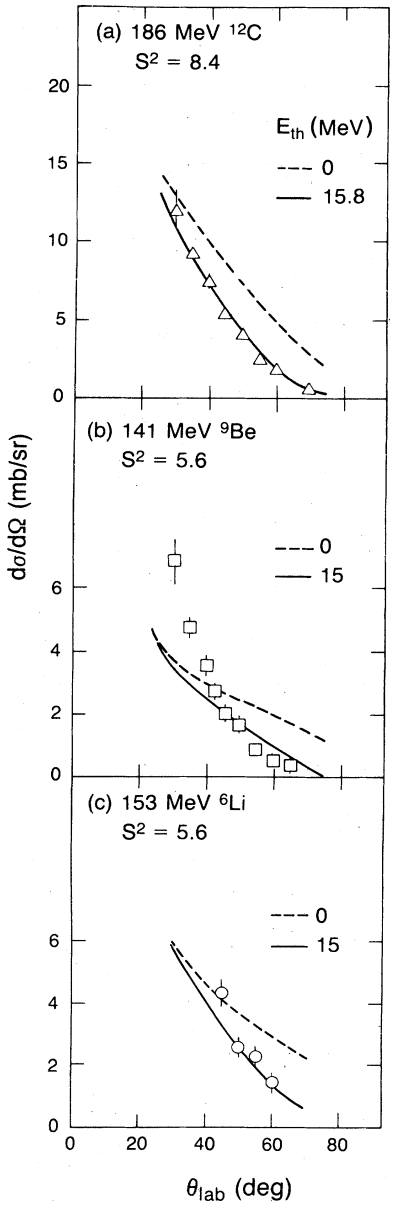

FIG. 10. Inclusive laboratory angular distributions for symmetric products from (a) 186 MeV ^{12}C, (b) 141 MeV ^{9}Be, and (c) 153 MeV ^{6}Li+^{40}Ca. The curves are Monte Carlo angular distributions calculated with (solid) and without (dashed) the experimental energy cutoff, E_{th}, and values of $E'^{c.m.}_{kin}=16.7$, 15.0, and 14.3 MeV for (a), (b), and (c), respectively.

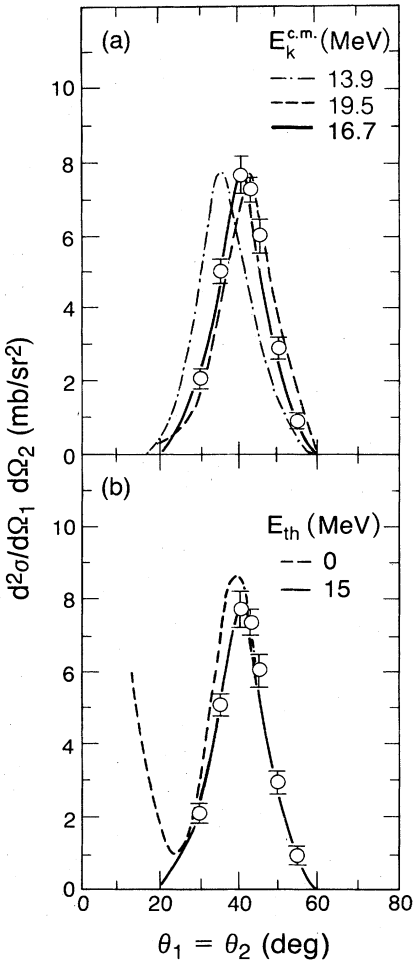

FIG. 11. Angular correlation ($\theta_1=\theta_2$) of symmetric products for the 186 MeV ^{12}C+^{40}Ca system. The curves are Monte Carlo calculations showing the dependence of the maximum in the correlation on (a) the c.m. kinetic energy and (b) the experimental cutoff. The effect of the lower energy cutoff is small.

and target nuclei and E_p is the incident energy. In our coincidence experiment, we measure θ_{ss}, the position of the maximum in the correlation curve, $\theta_1=\theta_2$. As can be seen from Fig. 6(a) the position of this maximum is not very sensitive to the value of S^2. It is also relatively insensitive to the value of the experimental energy cutoff [see Fig. 11(b)]. Consequently, one can conclude that

$$\theta_{ss}\simeq\theta'_{ss}\ . \tag{6}$$

The determination of $E'^{c.m.}_{kin}$ from the measured value of θ_{ss} using Eq. (5), and from a fit of the Monte Carlo calculations to the singles energy and coincidence distributions leads to similar results (see Table II).

C. Cross sections

The total cross section σ_f for the symmetric mass split was obtained by normalizing the Monte Carlo curve to the experimental angular distribution [Eq. (2)], or to the experimental angular correlation [Eq. (3)]. Operationally, the symmetric mass split was defined to be the yield in a bin three charge units wide centered at $Z_{sym}=\frac{1}{2}(Z_p+Z_T-\Delta Z)$, where ΔZ was the average charge loss due to evaporation. Table III contains values of σ_f obtained from both the coincidence and singles measurements. Figure 12 presents the energy dependence of σ_f measured for the ^{12}C+^{40}Ca system over the bombarding range of 74–186 MeV. For this reaction the symmetric yield deduced from the singles and coincidence data agrees within the errors. On the other hand, the ^{9}Be+^{40}Ca and ^{6}Li+^{40}Ca inclusive results exceed the coincidence cross sections by factors of 2 and 4, respectively. This indicates

TABLE III. The σ_f cross section for products in a bin three charge units wide centered at symmetry from coincidence and from singles measurements.

Reaction	σ_f (mb) (coincidences)	σ_f (mb) (singles)
$^{12}C+^{40}Ca$, 186 MeV	21.6±3.4	27.7±4.2
121.2 MeV	17.2±6.8	16.5±3.6
184.7 MeV		25.9±5.9
161.9 MeV		23.3±5.4
131.9 MeV		12.9±3.4
74.3 MeV		2.2±0.5
$^{9}Be+^{40}Ca$, 141 MeV	6.1±1.2	11.6±1.7
$^{6}Li+^{40}Ca$, 153 MeV	5.6±1.4	21.9±3.5

that the singles data for these latter reactions have contributions from processes other than symmetric splitting of an equilibrated system. These other processes seem to be stronger at forward angles [Figs. 10(b) and (c)] for the $^{6}Li,^{9}Be+^{40}Ca$ systems and at lower incident energies (Fig. 4) for the $^{12}C+^{40}Ca$ system.

IV. DISCUSSION

The measurements presented in this work clearly demonstrate the existence of symmetric or nearly symmetric decay of the three light systems investigated: $^{12}C+^{40}Ca\rightarrow{}^{52}_{26}Fe^*$, $^{9}Be+^{40}Ca\rightarrow{}^{49}_{24}Cr^*$, and $^{6}Li+^{40}Ca\rightarrow{}^{46}_{23}V^*$. The corresponding cross sections for the symmetric decay decrease from about 27 mb/3Z for $^{12}C+^{40}Ca$ at 186 MeV to about 6 mb/3Z for $^{6}Li+^{40}Ca$ at 153 MeV (see Table III).

The excitation function for the $^{12}C+^{40}Ca\rightarrow$symmetric products reaction exhibits a rapid increase with bombarding energy and then flattens out at higher energies (see Fig. 12). Such a dependence is suggestive of a compound nucleus process. Additional evidence that an equilibrated process is responsible for at least a large fraction of these symmetric products comes from the angular distributions. The higher energy $^{12}C+^{40}Ca$ data, which are less susceptible to contamination problems, are consistent with the angular distribution expected from the decay of a long lived composite system ($1/\sin\theta_{c.m.}$ in the vicinity of 90°).

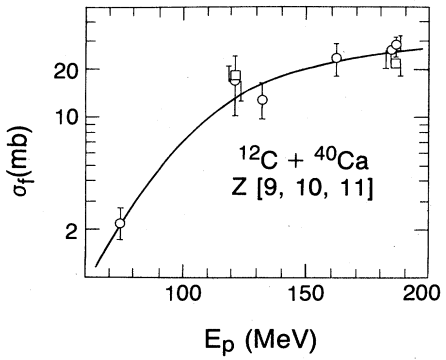

FIG. 12. Measured cross section of symmetric products ($Z=9-11$) from the $^{12}C+^{40}Ca$ reaction for several bombarding energies. The circles represent inclusive measurements and the squares coincidence measurements. The solid line is drawn through data points in order to guide the eye.

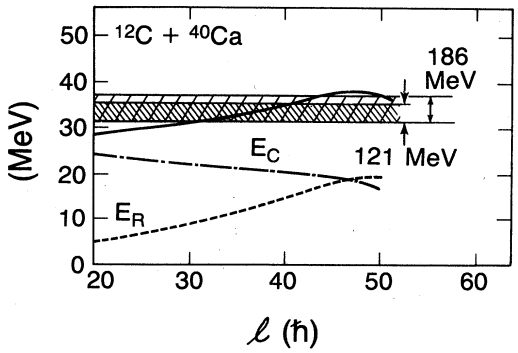

FIG. 13. Comparison of the extracted primary total kinetic energy for both the 186 and 121 MeV $^{12}C+^{40}Ca$ reactions (hatched areas) to a liquid drop model calculation (Ref. 14). The separate contributions for the Coulomb and rotational energies are indicated by dashed curves. The calculated total kinetic energy is indicated by the solid curve. Note the suppressed zero on the abscissa.

These systems are characterized by high fission barriers. Since angular momentum enhances the fission probability, one expects that the l-wave distribution responsible for symmetric splitting must be weighted toward the higher incident angular momenta. For these systems, the critical angular momentum for complete fusion (l_{CF}) is approximately 30$\hbar$,[12] while the grazing angular momenta (l_{gr}) vary from 53$\hbar$ for $^{12}C+^{40}Ca$ at 186 MeV to 30$\hbar$ at 74.3 MeV. If these symmetric products originate from true compound nuclei, the mean l wave should be less than but near the critical value. On the other hand, the l-wave region between l_{CF} and l_{gr} may also be responsible for producing these fragments if there is a significant probability for a composite system to form and survive long enough to diffuse towards mass symmetry and to rotate sufficiently to yield a $1/\sin\theta_{c.m.}$ angular distribution.

Evidence that the higher l waves are responsible for the production of these fragments is also apparent from the measured kinetic energies. In Fig. 13 the experimental total kinetic energies or TKE (crossed hatched areas) are compared to liquid-drop model calculations.[13,14] Since the saddle-to-scission energy is negligible in this region, the TKE is made up of the Coulomb (E_C) and relative rotational (E_R) energies at the saddle point. As the angular momentum is increased, the saddle point stretches, reducing the Coulomb energy. However, due to the small moment of inertia of the light systems, the reduction in Coulomb energy is more than compensated for by the increase in rotational energy. As a result the predicted total kinetic energy increases with l wave, and becomes consistent with the data for $l \geq 30$. The importance of the ro-

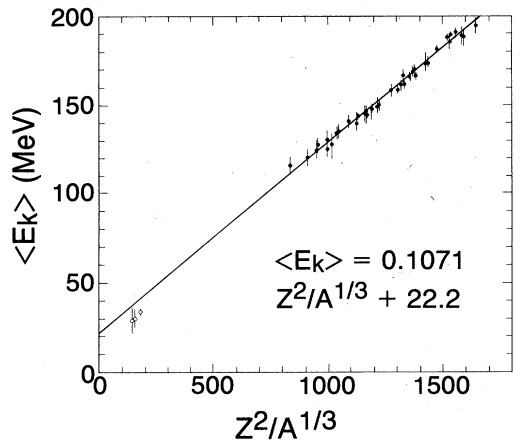

FIG. 14. Total kinetic energy for fission as a function of $Z^2/A^{1/3}$ of the composite system. The data of Viola (Ref. 18) (solid circles) are in the upper right of the figure and the data from the present work (open circles) are shown in the lower left. The solid line is a fit (Ref. 18) to the data of Viola (see the text).

tational energy term in the TKE for light systems has been established previously by Natowitz and co-workers for deep inelastic reactions.[15,16]

It is also of interest to compare the TKE of these symmetric products to standard fission systematics. Viola and Sikkeland have measured $E'^{\text{c.m.}}_{\text{kin}}$ for a number of nuclei between the rare earth and uranium region. The least square analysis of their and other available data[16,17,18] gives

$$2E'^{\text{c.m.}}_{\text{kin}} = 0.1071Z^2/A^{1/3} + 22.2 \text{ MeV} . \quad (7)$$

Here Z and A are the atomic and mass numbers of the composite system. According to Viola and Sikkeland this result is consistent with scission shapes corresponding to spheroids whose shapes minimize the total energy of the system.

For a system with $Z=0$, the total kinetic energy release should also be zero. Thus the Viola systematics, which were determined for large values of $Z^2/A^{1/3}$ and predict a substantial nonzero value for the total kinetic energy release at $Z^2/A^{1/3}=0$, must fail at small values of $Z^2/A^{1/3}$ like the present case. Nevertheless, it is interesting to see at what value of $Z^2/A^{1/3}$ the Viola systematics begin to deviate from the experimental data. The values of $2E'^{\text{c.m.}}_{\text{kin}}$ measured in this work are plotted in Fig. 14 together with the data of Viola and Sikkeland. In fact, the values of $2E'^{\text{c.m.}}_{\text{kin}}$ measured in this work fall 20—30% below the best fit line to the data of Viola and Sikkeland.

In summary, we have verified the existence of symmetric splitting for very light systems by utilizing coincidence techniques. The angular distributions imply a lifetime for the intermediate system equal to or greater than a rotational period. The measured excitation function for the $^{12}C+^{40}Ca$ system is consistent with compound nucleus decay. Comparison of the experimental kinetic energies to liquid-drop model calculations indicate that the l waves responsible for these symmetric splittings are greater than $\sim 30\hbar$.

ACKNOWLEDGMENTS

Three of the authors (K.G., Z.M., and R.P.) would like to thank the Nuclear Science Division for the support and hospitality received during their visits at the Lawrence Berkeley Laboratory. This work was supported by the U.S. Department of Energy under Contract DE-AC03-76SF00098.

*Permanent address: Universitá Degli Studi Di Bari, 70100 Bari, Italy.

†Permanent address: National Superconducting Cyclotron Laboratory, Michigan State University, East Lansing, MI 48824.

‡Permanent address: Chemistry Department, Washington University, St. Louis, MO 63130.

§Permanent address: Weizmann Institute of Science, Rehovot 76100, Israel.

[1]U. L. Businaro and S. Gallone, Nuovo Cimento 1, 629 (1955); 1, 1277 (1955).

[2]L. G. Moretto, Nucl. Phys. **A247**, 211 (1975).

[3]H. Oeschler, P. Wagner, J. P. Coffin, P. Engelstein, and B. Heusch, Phys. Lett. **87B**, 193 (1979).

[4]G. Guillarme, J. P. Coffin, F. Rami, P. Engelstein, B. Heusch, P. Wagner, P. Fintz, J. Barrette, and H. E. Wagner, Phys. Rev. C **26**, 2458 (1982).

[5]R. Holub, M. Fowler, L. Yaffe, and A. Zeller, Nucl. Phys. **A288**, 291 (1977).

[6]P. David, J. Debrus, H. Fahlbusch, and J. Schulze, Nucl. Phys. **A319**, 205 (1979).

[7]R. Eggers, M. N. Namboodiri, P. Gonthier, and J. B. Natowitz, Cyclotron Institute, Texas A&M University Report, 1980 (unpublished).

[8]J. Brzychczyk, L. Freindl, K. Grotowski, Z. Majka, S. Micek, R. Płaneta, M. Albinska, J. Buschman, H. Klewe-Nebenius, H. J. Gils, H. Rebel, and S. Zagromski, Nucl. Phys. **A417**, 174 (1984).

[9]L. G. Moretto, S. K. Kataria, R. C. Jared, R. Schmitt, and S. G. Thompson, Nucl. Phys. **A255**, 491 (1975).

[10]J. Gomez del Campo, R. G. Stokstad, J. A. Biggerstaff, R. A. Dayras, A. H. Snell, and P. H. Stelson, Phys. Rev. C **19**, 2170 (1970).

[11]T. Sikkeland and V. E. Viola, Jr., in *Proceedings of the Third Conference on Reactions Between Complex Nuclei,* edited by A. Ghiorso, R. M. Diamond, and H. E. Conzett (University of California, Berkeley, 1963), p. 232.

[12]W. Wilcke, J. R. Birkelund, H. J. Wollersheim, A. D. Hoover, J. R. Huizenga, W. U. Schröder, and L. E. Tubbs, At. Data Nuclear Data Tables **25**, 389 (1980).

[13]S. Cohen, F. Plasil, and W. J. Swiatecki, Ann. Phys. (N.Y.) **82**, 557 (1974).

[14]J. B. Błocki and W. J. Swiatecki, Lawrence Berkeley Laboratory Report 12811, 1982.

[15]R. Eggers, M. N. Namboodiri, P. Gonthier, K. Geoffroy, and J. B. Natowitz, Phys. Rev. Lett. **37**, 324 (1976).

[16]J. B. Natowitz, M. N. Namboodiri, R. Eggers, P. Gonthier, K. Geoffroy, R. Hanus, C. Towsley, and K. Das, Nucl. Phys. **A277**, 477 (1977).

[17]V. E. Viola, Jr. and T. Sikkeland, Phys. Rev. **130**, 2044 (1963).

[18]V. E. Viola, Jr., Nucl. Data Tables **A1**, 391 (1966).